

Supporting information

Anisotropic ionic conductivities in lyotropic supramolecular liquid crystals

Youju Huang, Yuanhua Cong, Junjun Li, Daoliang Wang, Jingtuo Zhang, Lu Xu,

Weili Li, Liangbin Li*, Guoqiang Pan

National Synchrotron Radiation Lab and Department of Polymer Science and Engineering, University of Science and Technology of China, Hefei, China

Chuanlu Yang*

Department of Physics and Electrons, Ludong University, Yantai, China

Materials

N, N'-dimethylacetamide (DMAc) was distilled under reduced pressure over magnesium sulfate and stored over molecular sieves (4 Å). 1, 3, 5-benzenetricarbonyl trichloride and 5-nitroisophthalic acid were purchased from Alfa Aesar and used as received without further purification. All other commercially available chemicals were purchased from Shanghai Chemical Reagents Co.

Part 1

Synthesis of compound 1

(4,4'-[(5-nitrobenzene-1,3-diyl)bis(carbonylimino)]dibenzenesulfonic acid)

5-nitroisophthalic acid (10.55 g, 0.05 mol), triphenyl phosphite (TPP) (30 mL) and Pyridine (25 mL) were dissolved in 200 mL of N,N-dimethylacetamide (DMAc)

• corresponding author: lbli@ustc.edu.cn, yangchuanlu@263.net

in a 500 mL three-neck round-bottomed flask equipped with a magnetic stirring bar. The mixture was then warmed up to 75 °C followed by the addition of 4-Anilinesulfonic acid (17.31 g, 0.1 mol) after 30 minutes under a N₂ atmosphere. At this time the temperature was increased to 115 °C. After 4 hours the mixture was precipitated in acetone and filtrated. The obtained solid was washed with ethanol and acetone several times, and then dried in the vacuum oven 80°C for 24 hours to give compound 1 (24.7 g, 94.7% yield). IR: 3100, 2966, 1684, 1623, 1592, 1529, 1486, 1398, 1354, 1229, 1119, 865, 832, 689 cm⁻¹. ¹H NMR (300 MHz, δ ppm, DMSO-*d*₆): 10.77 (s, 1H), 8.93 (m, 4H), 8.55(t, 2H), 8.02 (t, 2H), 7.73-7.62 (m, 4H). ¹³C NMR (67.5 MHz, DMSO-*d*₆) δ ppm = 127.3, 127.9, 133.3, 135, 141.4, 142.6, 146.6, 148.2, 164.8.

Synthesis of compound 2

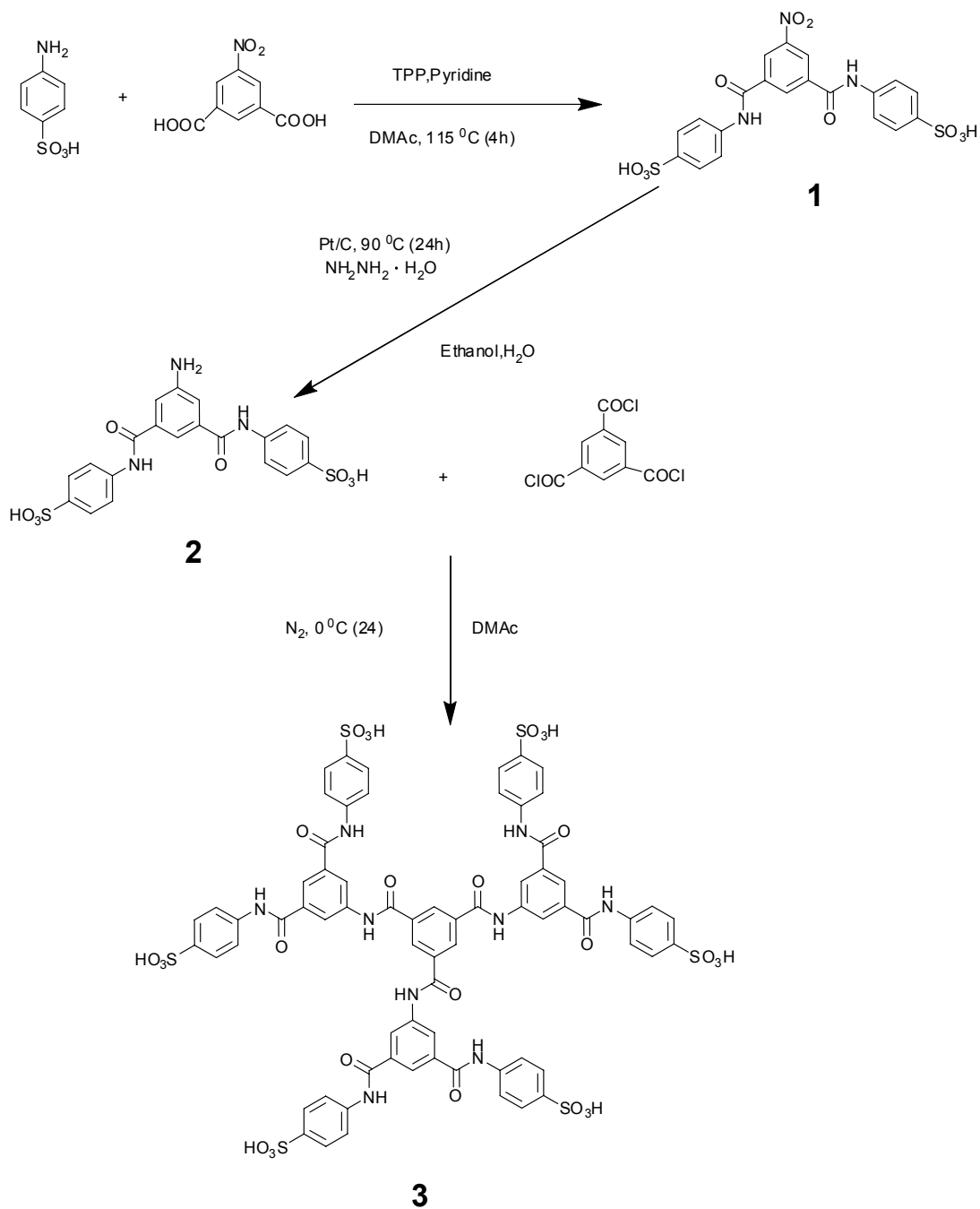
(4,4'-[(5-aminobenzene-1,3-diyl)bis(carbonylimino)]dibenzenesulfonic acid)

A 250 mL of three-neck round-bottomed flask were charged 10.0 g (19.17 mmol) of compound 1, 70 mL of distilled water and 70 mL of ethanol, with stirring under nitrogen flow. Then 0.5 g of palladium/activated carbon was added. When the reaction temperature was raised to 90 °C, 20 mL of hydrazine monohydrate was added dropwise. After hydrazine monohydrate solution was completely added, the reaction was kept at this temperature for 20 hours. After cooling to room temperature, the mixture was filtered. Then the filtrate was distilled under reduced pressure and the residual mixture was poured into 500 mL acetone, and the precipitate was filtered off, washed with ethanol and acetone several times, and then dried in the vacuum oven 80°C for 24 hours to give compound 2 (8.19 g, 86.9% yield). IR: 3438, 2975, 1653,

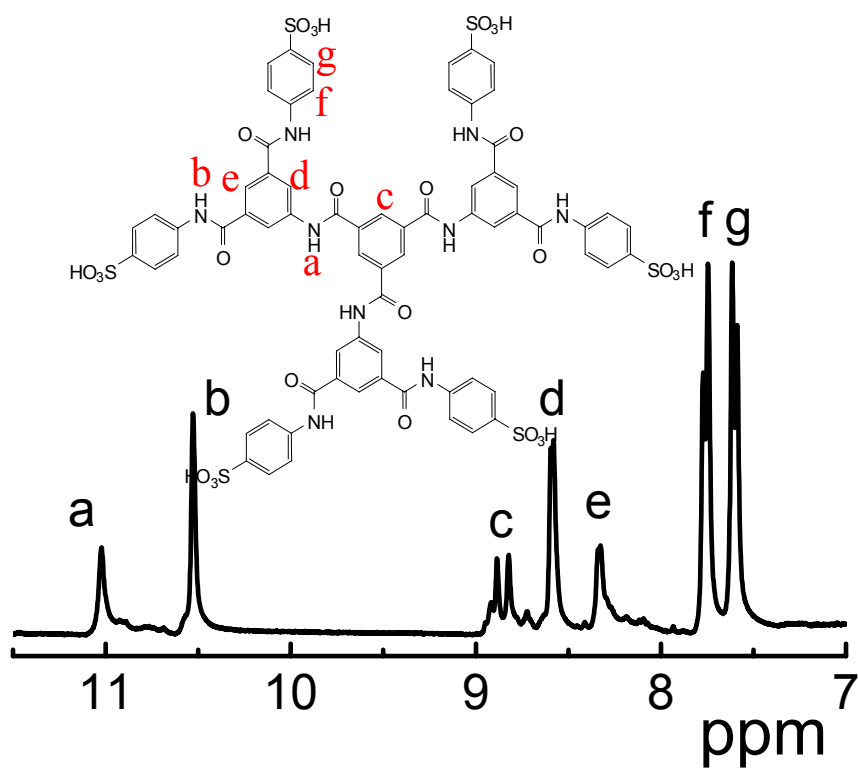
1594, 1529, 1445, 1398, 1338, 1229, 1124, 895, 837, 690. ^1H NMR (300 MHz, δ ppm, DMSO-*d*₆): 10.29 (s, 1H), 7.71 (t, 4H), 7.55 (d, 4H), 7.27 (s, 2H), 7.11 (s, 1H), 3.37 (s, 2H, -NH₂). ^{13}C NMR (67.5 MHz, DMSO-*d*₆) δ ppm=119.6, 126.1, 126.9, 133.0, 136.5, 138.7, 143.9, 147.8, 162.9.

Synthesis of compound 3 (the discotic molecule)

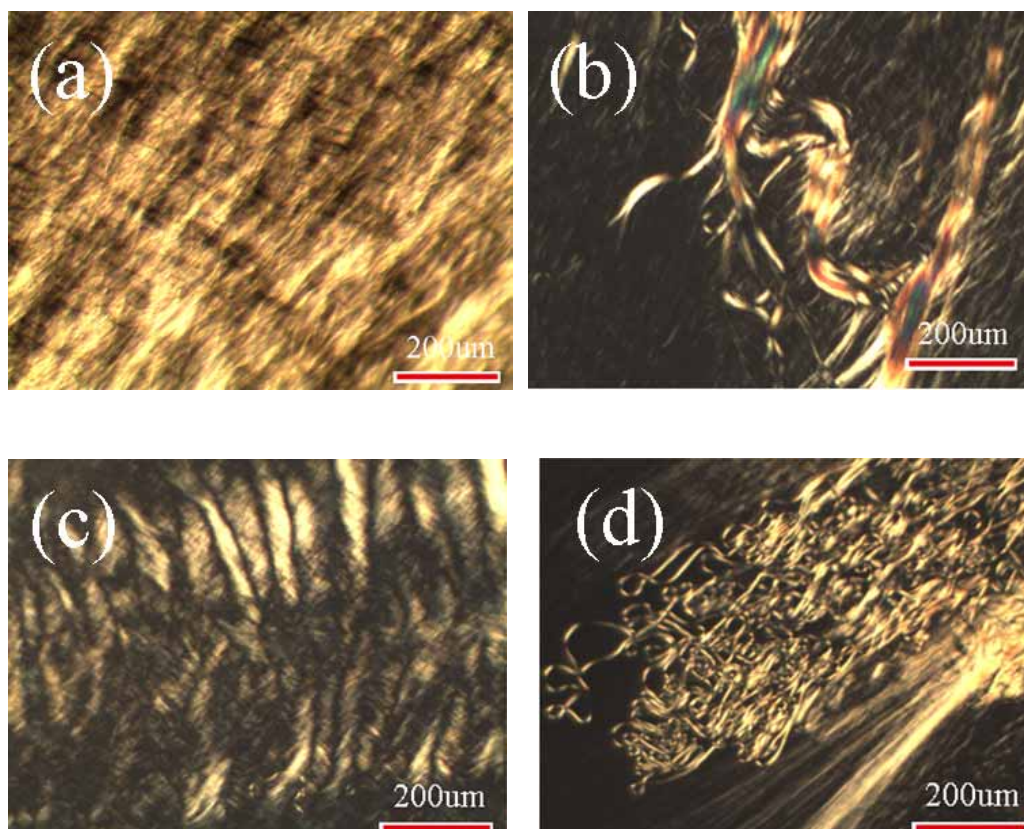
2.44 g (5 mmol) of compound 2 was dissolved in 100 mL of N, N-dimethylacetamide (DMAc) in a 250 mL three-neck round-bottomed flask equipped with a magnetic stirring bar under nitrogen flow. After the mixture was cooled in an ice bath to 0 °C, 0.442 g (1.67mmol) of 1, 3, 5-benzenetricarbonyl trichloride in 10 mL of DMAc was added to the solution under vigorous stirring. The reaction mixture was kept in an ice bath for 24 hours at room temperature and for another 2 hours at 60 °C. After cooling to room temperature, the mixture was distilled under reduced pressure and the residual mixture was poured into 300 mL acetone, and the precipitate was filtered off, washed with ethanol and acetone several times, and then dried in the vacuum oven 80°C for 24 hours to give compound 3 (2.19 g, 80.5% yield). IR: 3102, 1675, 1595, 1529, 1449, 1398, 1338, 1243, 1211, 837, 738, 685. ^1H NMR (300 MHz, δ ppm, DMSO-*d*₆): 11.01 (s, 3H), 10.52 (s, 6H), 8.72-8.91 (m, 3H), 8.57 (d, 6H), 8.32 (s, 3H), 7.74 (d, 12H), 7.60 (d, 12H). ^{13}C NMR (67.5 MHz, DMSO-*d*₆) δ ppm=119.3, 122.0, 122.7, 126.1, 135.2, 135.8, 139.1, 143.6, 165.0, 169.6. EI-TOF MS: calcd for (C₆₉H₅₁N₉O₂₇S₆-H)⁻:1629.58; Found: *m/z* 1629.50. Elemental analysis calcd (%) for C₆₉H₅₁N₉O₂₇S₆: C, 50.82; H, 3.15; N, 7.73; found: C, 50.80; H, 3.18; N, 7.79;

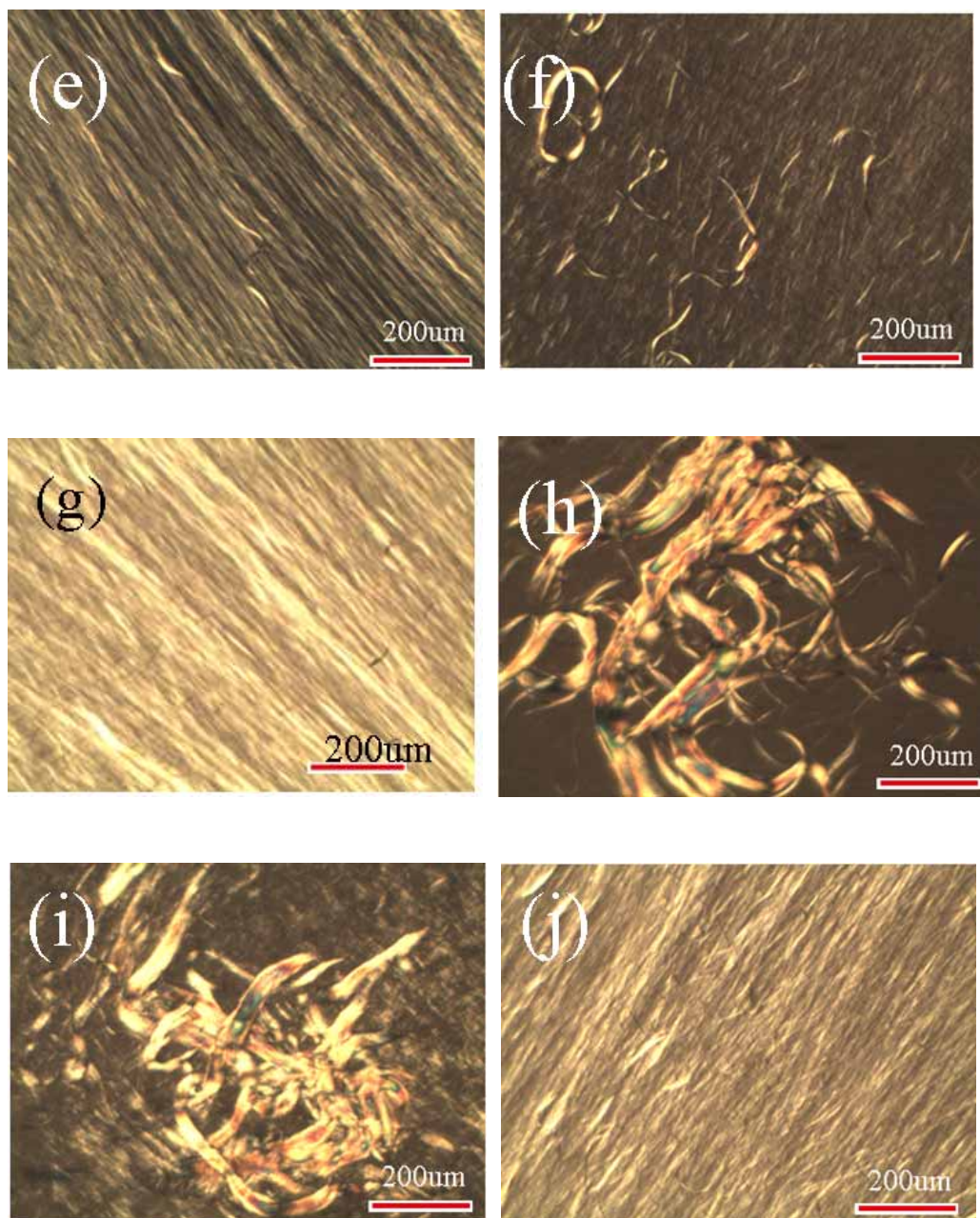


S-Scheme 1. Synthesis of the discotic molecule

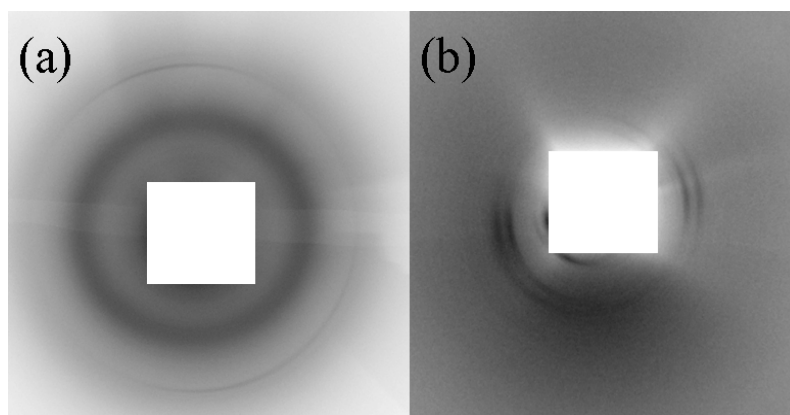


S-Figure 1. The $^1\text{H-NMR}$ of the discotic molecule





S-Figure 2. Polarized optical photomicrographs of the discotic molecule with different concentrations in water: (a) 0.086g/mL; (b) 0.087 g/mL; (c) 0.114 g/mL; (d) 0.114 g/mL; (e) 0.158 g/mL; (f) 0.176 g/mL; (g) 0.206 g/mL; (h) 0.206 g/mL; (i) 0.256 g/mL; (j) 0.280 g/mL. Note the liquid crystalline phase is easy to be aligned, which can be achieved by tilting the slide or shearing the samples.

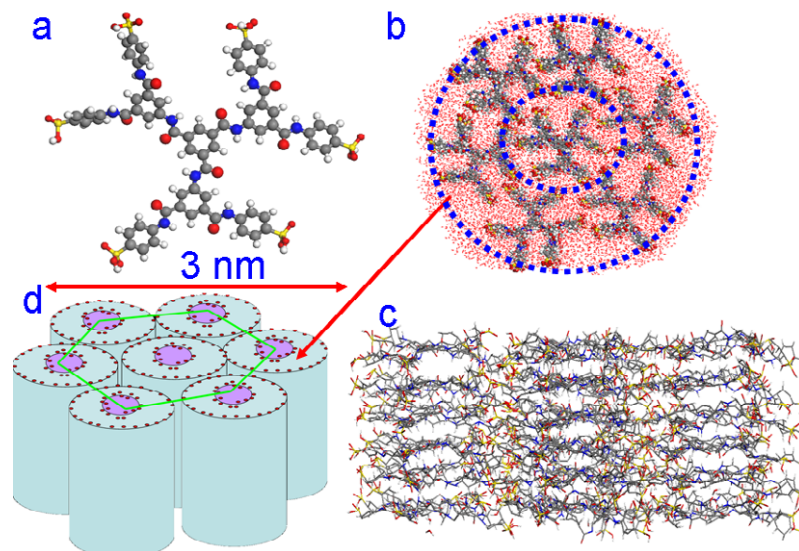


S-Figure 3. 2D patterns of the orientated discotic molecule with concentration of 0.206g/mL in the WAXS region (a), in the SAXS (b) region. The sample was aligned before measurements. As the area of the imaging plate can not cover SAXS and WAXS information at one sample to detector distance, the sample to detector distance was set at 400 mm and 170 mm to measure the SAXS and WAXS data, respectively, during which the sample was fixed on the sample holder without any movement. Note in the WAXS pattern the diffusion ring is the scattering from water. The scattering peaks at low q are orthogonal to the scattering peak in wide angle, which can be seen from the azimuthal intensity of scattering distribution.

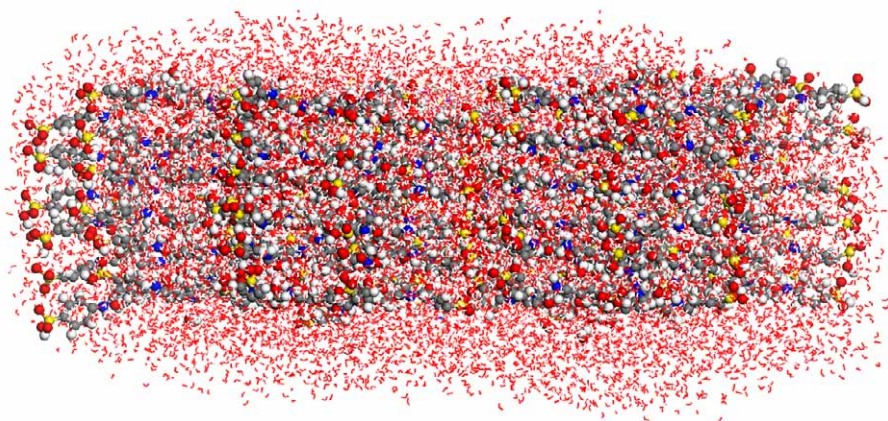
Part 2. The computer simulation

The calculations for the single discotic molecule are performed using the spin polarized density functional theory (DFT) ^[1] with the generalized gradient approximation (GGA) in “PW91” form. The molecular DFT DMol³ package is employed, in which double-numeric quality basis with polarization functions (DNP) that includes all occupied atomic orbital plus a second set of valence atomic orbital plus polarized d-valence orbital was chosen to describe the electronic wave functions.

It is a set of standard basis set in the package, providing reasonable accuracy for modest computational cost. In order to obtain reliable geometry of the molecule, all electron basis set and a strict convergent standard (the total energy is converged to 10^{-5} Hartree in the self-consistent loop and the force on each atom is less than 5×10^{-4} Hartree/Bohr) are employed although the total atoms reach 162 and the calculations are very time-consuming. The structure of multilayer are optimized using Conjugate Gradient (CG) (Fletcher_Reeves) method. The interactions among the atoms are described by consistent-valence force field (CVFF)^[2]. The minimization is successful completion when the maximum derivative is smaller than 0.001 Kcal/(mol·Å). All the calculations are performed using DISCOVER module in Material Studio 3.2. The optimizations are divided into three steps. Firstly, we constructed a model of a single discotic molecule. Secondly, a larger model including 7 model A (i.e. 7 discotic molecules and 2310 H₂O molecules) is constructed and optimized. Finally, model C (48384 atoms in total) containing 6-layer of model B is constructed and optimize). Nevertheless, the force field in the simulation does not account detailed specific interactions, which imposes some limitations on the simulation result. With large atom number and complex interactions, simulation based on first principle is still a challenge to current computing powder.



S-Figure 4. a) DFT optimized structure of the discotic molecule; b) The top view and the side view c) of the optimized structure of the column containing the discotic molecules and waters (CVFF and CG method); water molecules are omitted for a better view of the layers. d) Hexagonal packing of the columns highlighted the distribution of sulfonic acid groups of the discotic molecules.



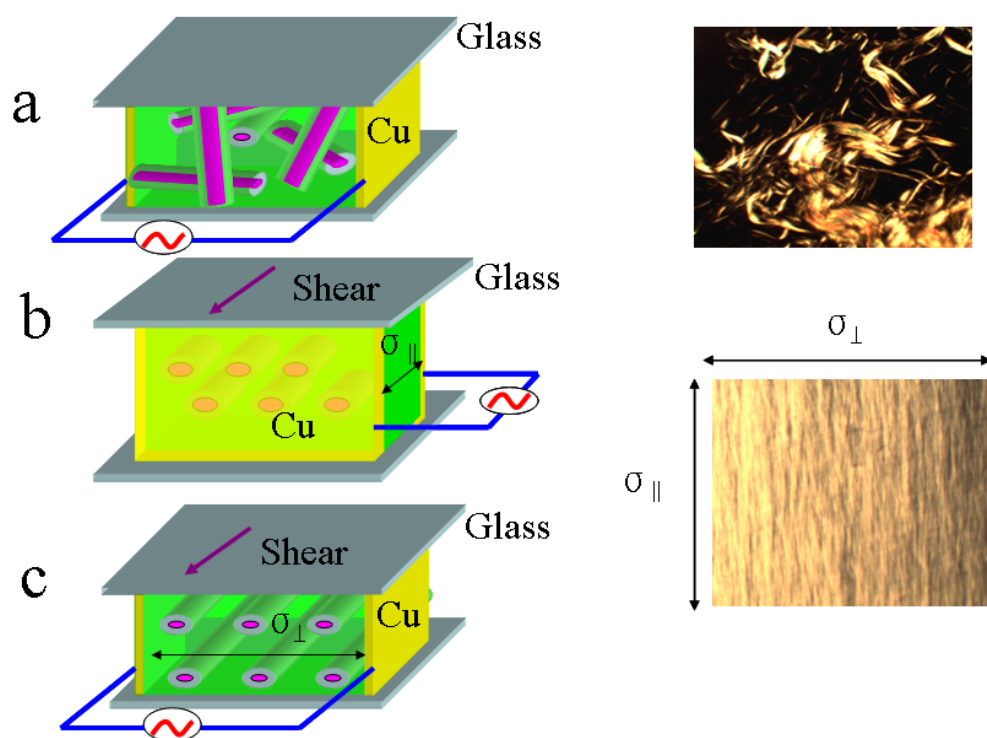
S-Figure 5. The side view of the optimized structure of the column containing the discotic molecules and waters (CVFF and CG method)

In order to elucidate how the column is constructed with the discotic molecules, we employed computer simulation to search the possible structure. With consistent-valence forcefield (CVFF) and conjugate gradient (Fletcher_Reeves) (CG) minimizer implemented in Discover module of Material Studio, the simulation shows that each layer of columns is formed by seven discotic molecules plus the interacted water molecules. The layers stack into a relative stable column, which has a diameter of about 8.7 nm (S-Figure 4b top view and S-Figure 4c side view). If we take into account the water molecules around the columns, this value is very reasonable for the d spacing of the hexagonal columnar liquid crystals. In order to get a better view of the layers of the hexagonal columnar liquid crystals, the water molecules are not shown in the side view picture. The image with water was shown in the S-Figure 5. The layer spacing from the computer simulation is in good agreement with the layer spacing of WAXS data, which is close to 0.35 nm due to the π - π stack instead of hydrogen bonding. Thus the main driving force for the formation of columnar structures can be π - π interactions between the phenyl rings, which is reasonable as the hydrogen bonds can form between water and the amide groups.

Looking close at the column of hexagonal supramolecular liquid crystalline phase, we observed that the sulfonic acid groups at the periphery of the discotic molecules tend to self-organize into two coaxial proton nanochannels. The inner nanochannel is circumambient at the periphery of the interior discotic molecule, while the outer one surrounds the columns of the hexagonal supramolecular liquid crystalline phase, as highlighted in S-Figure 4b with the dash line. As the outer channels were connected

with each other, they are an open ionic channel. Thanks to the novel layer structure of the column with seven discotic molecules, the inner channels were isolated by the phenyl rings, which is a relatively closed ionic nanochannel. As these columns with coaxial proton channels further form hexagonal liquid crystalline phase (S-Figure 4 d, a red dot represent a sulfonic acid group, only the distribution of sulfonic acid groups of a layer was shown in the S-Figure 4d), the ionic channels can be easily aligned into macroscopic uniform orientation (see Figure 1b), whose ionic conductivity is expected to be anisotropic.

Part 3



S-Figure 6. ((Illustrations of cells for the measurements of ionic conductivities of (a) random oriented columnar phase (b) Parallel to columnar orientation of discotic liquid crystals (c) Perpendicular to columnar orientation of discotic liquid crystals.

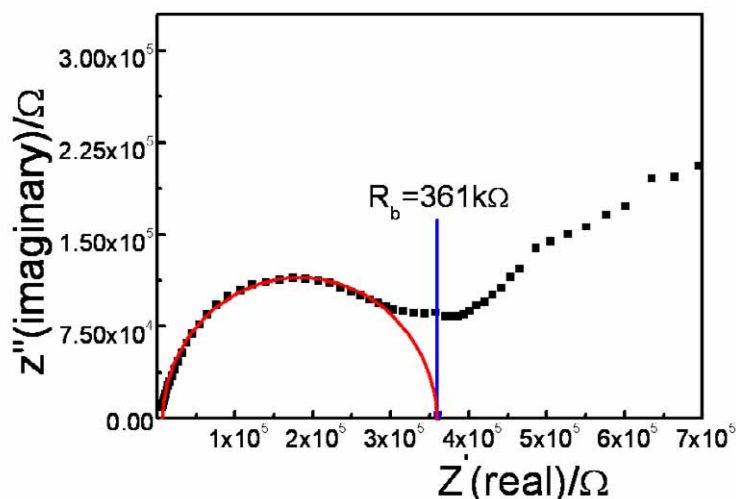
Before measuring the ionic conductivities of discotic liquid crystals, the columnar orientations of discotic liquid crystals were checked by the POM.)

Measurements of Ionic Conductivities

Ionic conductivities were measured by AC impedance method according to precious literature^[3] using CHI660C electrochemistry workstation (frequency range: 0.1Hz–100 KHz, applied voltage: 0.5 V). Ionic conductivities (σ) can be obtained from the following equation:

$$\sigma = d / (R_b A)$$

where R_b , d , and A are the bulk resistance, the sample thickness, and the cross sectional area of the electrode, respectively. Ionic conductivities were practically calculated to be the product of $1/R_b$ (Ω^{-1}) times cell constants (cm^{-1}), which were calibrated with KCl aqueous solution (0.1 mol L^{-1}) as a standard conductive solution. The impedance data (Z) were modeled as a connection of two RC circuits in series (R : resistance, C : capacitance) and was divided into real (Z') and imaginary (Z''). A representative example of an impedance spectrum exhibited by **1a** at room temperature is displayed in S-Figure 7. The bulk resistance R_b was obtained from the intercept of the left semi-circle on the Z' axis. These data were collected over a range of concentration to examine the concentration dependence of the ionic conductivity of the materials.

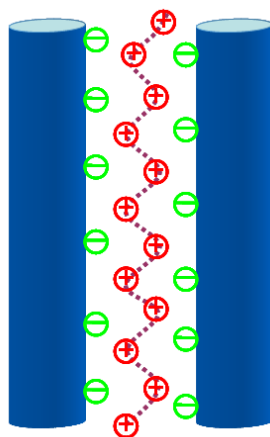


S-Figure 7. Impedance spectrum for the unoriented discotic molecule with a concentration of 0.185 g/mL in the columnar state at room temperature. The bulk resistance R_b was obtained from the intercept of the left semi-circle on the Z' axis.

Part 4

It is very interesting to find that the spacing of the (100) plane of the hexagonal liquid crystalline phase keeps relative constant in two concentration regions by the SAXS/WAXS data, which indicates a nonlinear correlation between the concentration and the d spacing. This can not be explained with the mean-field approaches of Debye-Hückel or Poisson-Boltzmann theory [4], though it can account the increase of d spacing with the decrease of concentration. The relative constant d spacing in the two sub-ranges of concentration certainly corresponds to local minima in free energy landscape. Clearly an attraction force should exist in the system, which prevents the d spacing from continuously decreasing. Attraction between like-charged rods has been observed in a variety of systems especially in biological materials like actins. In the last 30 years, a great of effort has been dedicated to interpret this phenomenon and

different models are proposed, which, however, does not reach a full agreement yet. [5, 6] Though the detailed physical pictures of different models may be slightly different, the essential ideas are rather similar as illustrated in S-Figure 8. In current case,



S-Figure 8. The schematic illustration of charge density distribution of two neighbor charged rods.

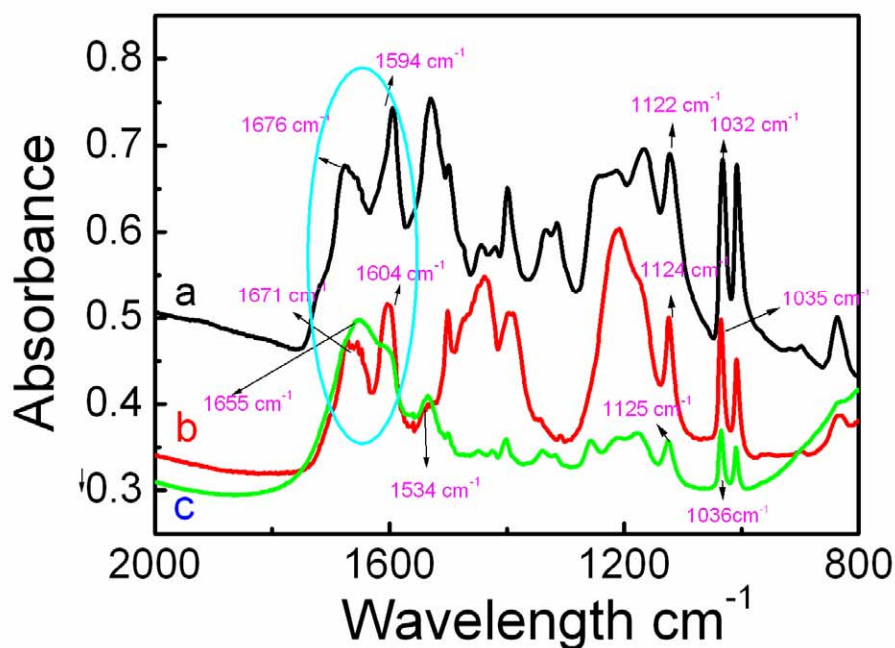
neighbor rods shift relatively about half layer spacing along the axis direction, which leads to the sulfonic groups from the neighbor rods mismatching in the axis direction. The counterion protons located between the rods follow similar shifting along the axis. Though the charges may not be completely fixed at certain positions, the distribution of ions leads to the formation of two anti-parallel charge density waves of anion and cation along the axis, respectively, which construct a “zipper-like” charge alignment and are the origin of the attractions between like charged rods. The attractions among the columns are all relatively short range, while the charged columns are mutually repulsive at long range. [7, 8] The competition between long range electrostatic repulsion and short ranged attractions results in the stable structure in the two ranges of concentrations. Based on the models for like charged rods, it is

possible to give a qualitative explanation on our experimental result. Nevertheless, as no full agreement is reached on the theory yet and the discotic molecules in the water contain nearly all secondary interactions such as hydrogen bonding, π - π interaction, hydrophobic and hydrophilic, electrostatic and van de Waals force, a quantitative interpretation on this phenomenon is still a challenge.

Part 5

Hydrogen bonds

IR spectra of the discotic molecule have been collected in Nicolet 8700 FT-IR spectrophotometer. Liquid cell is KRS-5 windows. All data are processed with OMNIC 5.2 software. FT-IR spectra of the discotic molecule, which was shown in the below S-Figure 9.



S-Figure 9. The FT-IR spectra of (a) dry sample of discotic molecule protected in the liquid paraffin oil, (b) the discotic molecule solution in D_2O with a

concentration 0.20 g/mL, (c) the discotic molecule solution in water with a concentration 0.20 g/mL.

Compared with S-Figure 9a and S-Figure 9b, the absorption of the C=O st (amide I) and N-C=O st (amide II) has an obvious shift, which is an evidence to prove the existence of interactions between the amide bonds and D of D₂O. Furthermore the absorption peaks of the C=O st (amide I) and N-C=O st (amide II) of discotic molecules in water (S-Figure 9c) have a significant shift and become broader, up to 1655 cm⁻¹ and 1534 cm⁻¹ respectively, which are in good agreement with the data formed hydrogen bonding between the amide bonds and water [9,10]. These entire phenomenons indicate the forming of hydrogen bonding between the amide bonds and water. Likewise, characteristic absorption peaks of sulfonate anion, SO₃⁻ (1125 and 1036 cm⁻¹) of S-Figure 9c indicate the forming of hydrogen bonding between the sulfonic acid groups and water or amide bonds.

Reference

- [1] B. Delley, *J. Chem. Phys.* 1990, **92**, 508-517.
- [2] Accelrys Materials Studio 3.2; *Accelrys Software, Inc.*: San Diego, 2005.
- [3] M. Yoshio, T. Kagata, T. Hoshino, T. Mukai, H. Ohno and T. Kato, *J. Am. Chem. Soc.*, 2006, **128**, 5570-5577.
- [4] Jensen, N. G.; Mashl, R.J.; Bruinsma, R. F.; Gelbart, W. M.; *Phys. Rev. Lett.* **1997**, 78, 2477
- [5] Kornyshev, A. A.; Lee, D. J.; Leikin, S.; Wynveen A. *Rev. Mod. Phys.*, **2007**, 79, 943

- [6] Golestanian, R.; Kardar, M.; Liverpool, T. B. *Phys. Rev. Lett.* **1999**, *82*, 4456.
- [7] Angelini, T.E.; Liang, H.J.; Wriggers, W.; Wong, G. C. L. *PNAS*, **2003**, *100*, 8634
- [8] Wong, G. C. L. *Curr Opin Colloid Interface Sci*, **2006**, *11*, 310.
- [9] Clark, R. J. H., Hester, R. H., *Advances in Infrared and Raman Spectroscopy*. Heyden & Son Ltd.: London, **1980**; Vol.5.
- [10] Ernö, P.; Philippe, B.; Martin, B. *Structure Determination of Organic Compounds: Tables of Spectral Data*. Springer-Verlag Berlin Heidelberg **2009**.